MULTI-OBJECTIVE EVOLUTIONARY OPTIMIZATION OF PASSIVE ENERGY DISSIPATION SYSTEMS UNDER SEISMIC LOADING

O. Lavan[1], G.F. Dargush[2] and A.M. Reinhorn[3]

[1] *Senior Lecturer, Faculty of Civil and Environmental Engineering , Technion Israel Institute of Technology, Haifa, Israel*

[2] *Professor, Dept. of Mechanical and Aerospace Engineering , University at Buffalo, Buffalo, NY, USA*

[3] *Professor, Dept. of Civil, Structural and Environmental Engineering , University at Buffalo, Buffalo, NY, USA*

Email: lavan@tx.technion.ac.il, gdargush@eng.buffalo.edu, Reinhorn@buffalo.edu,

ABSTRACT:

With the conceptual development of performance-based design, the earthquake engineering community has begun to recognize the importance of controlling both interstory drifts and absolute floor accelerations. However, these often present conflicting requirements for design. In this paper, we present a multi-objective genetic algorithm to address this conflict by identifying a Pareto front of optimal solutions. This provides decision makers with the information needed to understand the tradeoffs between the two objectives of minimizing drift and acceleration. Furthermore, the multi-objective approach allows broad comparisons between different types of structural response control strategies and devices. Here we focus on several passive energy dissipation systems, with particular emphasis on nonlinear viscous fluid dampers. In addition to presenting the overall multi-objective framework, we consider an example of a five story steel building and evolve some interesting Pareto front structural designs.

KEYWORDS:

Passive energy dissipation systems; Performance-based seismic design; Non-structural components; Structural optimization; Genetic algorithms; Pareto front

1. INTRODUCTION

There has been a significant shift in the approach to seismic design over the last decade. Many new technologies have been developed and refined. For example, passive energy dissipation systems (Soong and Dargush, 1997; Christopoulos and Filiatrault, 2006) have reached a considerable level of maturity. There also has been increased emphasis on the behavior of non-structural components (Villaverde, 1997a, b), especially in critical facilities. Furthermore, the overall concept of performance-based design (Bertero, 1997; Priestley, 2000) has gained prominence.

While all of this represents a major step forward, the design process itself has become increasingly complex as a result. Consequently, new approaches are needed to evaluate and compare systematically various design alternatives. For example, there is strong evidence to employ maximum inter-story drift as a simple measure for quantifying the performance of the primary structural system and some non-structural components. On the other hand, for many non-structural components and building contents, maximum absolute acceleration may represent a more pertinent measure. Thus, one can argue that design should focus on minimizing both of these two performance measures. Unfortunately, drift and acceleration often represent competing objectives under seismic excitation. Designs that provide small drifts may result in substantial accelerations and *vice versa*.

Meanwhile, the single objective sizing and placement problem for passive control devices under seismic excitation has received considerable attention and three distinct approaches have emerged. The simplest approach involves optimality criteria methods, such as the sequential placement algorithm proposed by Zhang and Soong (1992) and a fully-stressed design approach developed by Levy and Lavan (2006). Alternatively, one can adopt a mathematical programming approach, as long as the problem is restricted to differentiable functions. For example, Takewaki (1997), Singh and Moreschi (2001) and Lavan and Levy (2005) utilize gradient-based optimization methods. The third overall approach involves heuristic optimization algorithms, primarily genetic algorithms that have their basis in the work of Holland (1975). Genetic algorithms were applied initially to design linear dampers for linear structures in Furuya *et al.* (1998) and Singh and Moreschi (2002), while Liu *et al.* (2005) addressed the same problem with a hybrid method. The genetic algorithm approach is quite general and is in no way restricted to linear structures. Thus, optimal design of passive dampers for nonlinear structures has been addressed successfully using genetic algorithms by Moreschi and Singh (2003) for a suite of four synthetic earthquakes and in Dargush and Sant (2005), which considered an uncertain seismic environment and alternative damper types. However, all of these efforts address problems of single objective optimization. Here we develop an evolutionary approach for multi-objective optimization that simultaneously attempts to minimize interstory drifts and absolute floor accelerations by defining the Pareto front of design solutions.

2. MULTI-OBJECTIVE STRUCTURAL OPTIMIZATION

As discussed above, for buildings under seismic excitation, inter-story drift and story total acceleration become key measures for damage of the structural system, non-structural components and building contents. Consequently, minimization of these two measures within a multi-objective formulation can provide valuable information for performance-based seismic design.

In order to formulate the optimization problem for a structural system subjected to a suite of strong ground motions, let $\Delta_i^{(e)}(t)$ represent the inter-story drift at time t between the $i-1^{\text{st}}$ and i^{th} story during earthquake e, while $a_i^{(e)}(t)$ denotes the corresponding i^{th} story total acceleration. Then, for an N-story building, subjected to an ensemble of N_e earthquakes, define drift and acceleration performance measures

$$\Delta_{\max} = \max\left\{ \ |\Delta_i^{(e)}(t)| \quad \text{for} \quad i=1,\ldots,N;\ 0 \le t \le t_{\max}^{(e)};\ e=1,\ldots,N_e \right\} \tag{2.1a}$$

$$a_{\max} = \max\left\{ \ |a_i^{(e)}(t)| \quad \text{for} \quad i=1,\ldots,N;\ 0 \le t \le t_{\max}^{(e)};\ e=1,\ldots,N_e \right\} \tag{2.1b}$$

where $t_{\max}^{(e)}$ is the duration of earthquake e. Furthermore, define corresponding non-dimensional drift η and acceleration ξ performance measures, where $\eta = \Delta_{\max}/\Delta_{\lim}$ and $\xi = a_{\max}/a_{\lim}$. Here $\Delta_{\lim}$ and $a_{\lim}$ represent limiting values for the range of interest of inter-story drift and total story acceleration, respectively. Design, then, involves minimizing the two performance measures η and ξ.

These two distinct objectives are accommodated by employing the well-established notion of Pareto optimality (Pareto, 1927), an approach that can be particularly attractive for decision makers. With this approach, rather than attempting to identify a single optimal design, one seeks to determine the entire family of designs that lie on the Pareto front. In general, a Pareto front design represents a feasible solution for which an improvement in any objective can be realized only by accepting a degraded performance in at least one other objective. Thus, in the present context, for each Pareto front design, a reduction in maximum inter-story drift can be achieved only by accepting a feasible design with an increased value for maximum absolute story acceleration, and *vice versa*, as illustrated in Figure 1. Identification of the entire Pareto front presents the decision maker with a more complete picture of the potential design solutions and allows trade-offs between target values for maximum drift and acceleration to be considered.

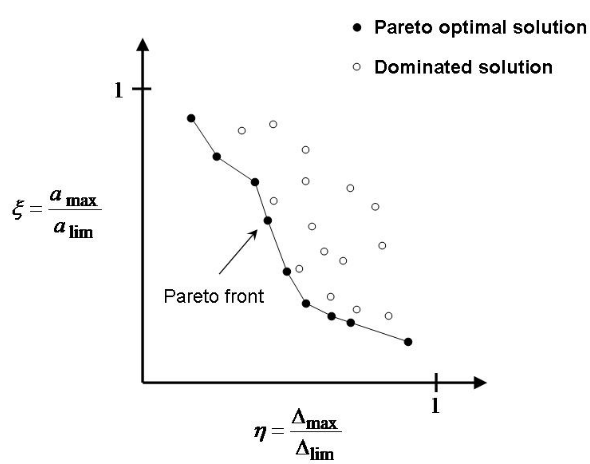

Figure 1 Pareto front definition

3. STRUCTURAL MODELS

Within the present multi-objective evolutionary framework, the basis for the fitness evaluation of each potential structural design is time-history dynamic analyses over a set of pre-defined ground motions. These dynamic analyses employ an explicit state-space approach, similar to that described in Dargush and Sant (2005).

The inertial properties of the bare structure are represented at each story by a lumped mass m_i associated with the total horizontal acceleration of story i with $i = 1, \ldots, N$ for an N-story building. Meanwhile, the stiffness of the primary structure is approximated by employing a lumped-parameter, kinematic-hardening, cyclic plasticity model for each story. The stiffness k_i, yield force f_{yi} and post-yield stiffness k_{yi} must be specified for each story. The current story force f_i and back-force b_i are included in the state-space formulation as internal variables, with the back-force used to track the center of the elastic domain in force-space. Mass and stiffness proportional Rayleigh damping is included.

For the passive dampers, three distinct types are considered, namely metallic buckling restrained braces, viscous fluid dampers and viscoelastic solid dampers. All three types are modeled using a lumped-parameter idealization at the appropriate story level. Multiple dampers within a given story are assumed to be of a single type and to act in parallel.

The buckling restrained braces (BRB) are represented by the same lumped-parameter, kinematic-hardening, cyclic plasticity model mentioned above. Thus, for any story in which metallic dampers are included, the BRB stiffness k_i^{BRB}, yield force f_{yi}^{BRB} and post-yield stiffness k_{yi}^{BRB} must be specified and the evolution of two internal variables (*i.e.*, f_i^{BRB}, b_i^{BRB}) are incorporated in the governing equations. Here the three parameters k_i^{BRB}, f_{yi}^{BRB} and k_{yi}^{BRB} are all assumed proportional to the cross-sectional area A_i^{BRB} of the brace. Consequently, only the single sizing parameter A_i^{BRB} is required for each story.

Linear viscous fluid (VF) dampers are assumed to provide damping forces f_i^V that are proportional to the horizontal inter-story drift rate $\dot{\Delta}_i$ with constant damping coefficient c_i^V. This implies that the dampers themselves are purely linear Newtonian devices and that the accompanying braces are infinitely stiff compared to the story stiffness of the primary structure. The effect of the brace orientation angle is assumed to be incorporated in c_i^V. A nonlinear power law viscous fluid damper (NVF) is also considered with exponent ν and damping coefficient c_i^V, which is established by equating forces to that in a linear viscous damper at a reference drift rate $\dot{\Delta}_{\text{ref}}$. This NVF damper is always assumed to act in series with an elastic brace of stiffness κk_1, where k_1 is the first story stiffness of the primary structure.

The model employed for the viscoelastic (VE) dampers accounts for both the frequency and temperature dependence of these devices. The solid viscoelastic layers of the damper are assumed to behave as thermo-rheologically simple (TRS) materials. A generalized Maxwell model with three relaxation times represents the shear response as a function of frequency, while a linear shift function models the effect of temperature. This not only allows for the change in response with ambient temperature, but also accounts for the loss of stiffness due to the internal heating associated with energy dissipation during a seismic event. Here ambient temperature is assumed to be 21.7°C and the layer thickness is set to restrict maximum shear strains in the VE device to approximately 100% under conditions of limiting inter-story drift Δ_{lim}. The only remaining model parameter, the shear area A_i^{VE}, then controls the size of the VE dampers in story i. Within the state-space formulation, five internal variables are introduced for each story that incorporates VE dampers. One internal variable is associated with each of the three Maxwell elements, another internal variable represents the damper temperature and the fifth internal variable monitors an intrinsic dimensionless time.

Whatever passive devices are employed within a given building, the resulting set of first order state-space equations can be written:

$$\dot{\mathbf{X}} = \mathbf{F}(\mathbf{X}, t) \tag{3.1}$$

where the dependent variables $\mathbf{X}$ include the horizontal story displacements and velocities, along with all of the internal variables required to describe the non-linear behavior of the primary structure and passive dampers. In the present implementation, Eqn 3.1 is solved using an explicit approach, based upon an embedded Runge-Kutta algorithm (Press *et al.*, 1992). This provides very efficient solutions with automated error control.

For the proposed multi-objective evolutionary design framework, base properties must be provided for each of the three potential passive devices. Thus, one must specify $\overline{A}^{BRB}$ for the buckling restrained braces, $\overline{c}^{V}$ for the linear and nonlinear viscous fluid dampers, and $\overline{A}^{VE}$ for the solid viscoelastic devices. For each story within a structural design, the actual damper size is defined by three parameters α_i, β_i and γ_i, which specify the sizing scale factors for buckling restrained braces, viscous fluid dampers and solid viscoelastic devices, respectively, in story i. For example, if buckling restrained braces are specified for the second story, then $A_2^{BRB} = \alpha_2 \overline{A}^{BRB}$ and $\beta_2 = \gamma_2 = 0$. Within the evolutionary algorithm, a binary code is utilized to represent α_i, β_i and γ_i for each story of the passively damped building. The concatenation of these individual story codes forms an overall structural design chromosome. The genetic algorithm uses a population of N_p structural design chromosomes, along with a series of genetic operators, to evolve Pareto optimal damper configurations over a sequence of N_g generations. A new algorithm, using local and global fitness measures, was developed to maintain diversity of the evolving population, but a full description cannot be given here.

4. COMPUTATIONAL EXAMPLE

A comprehensive study, involving a range of structures and seismic environments, would be required in order to provide general guidance for seismic design and retrofit. While the proposed evolutionary approach is ideally suited for such an investigation, this cannot be considered within the scope of the present paper. Instead, the primary objective here is to illustrate the proposed multi-objective evolutionary methodology via application to the five-story regular yielding shear frame shown in Figure 2a. For this example, four ground motion records (*i.e.*, $N_e = 4$) are considered, and the four different types of dampers discussed previously are taken into account in the retrofitting process. Thus, buckling restrained braces (BRB), linear viscous fluid dampers (VF), nonlinear viscous fluid dampers (NVF) and viscoelastic dampers (VE) are all considered. Furthermore, four sizing bits are used for the dampers (*i.e.*, $n_d = 4$), that is to say $N_d = 16$ distinct damper sizes are taken into account. Since multi-objective optimization is performed, a large range of damper sizes should be considered to cover the entire range of values for the different objectives. In addition, different damper sizes should be expected for the individual stories. The maximum size of damper is thus chosen based on the properties of the structure only, and is rather large with regard to its properties, as will be shown subsequently.

Then, each of the remaining sizes is a fraction of the maximum size, following a geometric progression: $z_l = z_{\max} \cdot \chi^{(l - N_d)}$; $l = 1, 2, ..., N_d$ where z_l is the l^{th} smallest damper size, $z_{\max}$ is the maximum damper size, and χ is the ratio between two adjacent sizes. In the examples, $\chi = 1.3$ for BRBs and $\chi = 1.2$ for VFs, NVFs and VEs.

The five story frame considered here has a uniformly distributed mass of 1.0 metric ton (*i.e.*, 1000 kg) per floor and was designed to have a linear first mode shape with a dominant period of 0.5 sec. The yield shear forces of the stories were then computed based on the maximum shear forces, experienced by the structure in an elastic time history analysis for the ground motions considered, divided by 4. A bi-linear hysteretic model with 2% kinematic hardening was adopted to represent the behavior of the restoring shear forces. Meanwhile, the ensemble of ground motions is comprised of four records from the LA10in50 ground motion ensemble (see Somerville *et al.* , 1997). The records LA13, LA14, LA16 and LA17 were chosen over other records in the LA10in50 ensemble, since these resulted in the largest drifts in the bare frame.

Since the frame was designed to have a linear first mode shape, the corresponding drifts are $\{1.00 \quad 1.00 \quad 1.00 \quad 1.00 \quad 1.00\}^T$. A damping distribution proportional to this vector and scaled by a factor of 138.2 kN·s/m was required to provide added damping at 50% of critical in the first mode. Hence, the maximum VF damper size was taken as 138.2 kN·s/m. The maximum stiffness of the BRBs was taken here as four times the stiffness of the stiffest story, or 4·2368.7=9475 kN/m. Evaluation of the yield drift of this damper leads to a yielding drift of the damper that is larger than that of the frame. This would defeat the purpose of the example. Hence, a value of 0.0047 m (*i.e.*, 50% of the yielding drift of the frame) is adopted. For the period of the structure and VE material used, the damping coefficient is given by 255.6*A*/*h* in SI units, where the shear viscosity is 255.6 kPa·s. Hence, a ratio of *A*/*h* equal to 0.5404 m was adopted to result in a damping coefficient of 138.2 kN·s/m for that frequency. The stiffness associated with this VE damper is 1098 kN/m, while its thickness was taken as 0.0668 m and its area as 0.0361 m^2.

The example was first run for three different cases, where BRB, VF and VE dampers were considered separately, using $N_p = 128$ and $N_g = 512$. For these cases, the limits on the inter-story drifts and total acceleration, which are required to determine η and ξ, are $\Delta_{\text{lim}} = 0.10$ m and $a_{\text{lim}} = 2.5$ g, respectively. The Pareto front approximations for all three of these cases are presented in Figure 2b, along with the response point for the bare frame. Notice that all three passive systems can provide significant reductions in drift compared to the bare frame. Accelerations also can be reduced, but to a lesser extent. Interestingly, for this example, Pareto optimal BRB and VE passive damper designs have quite similar performance over drift levels between $0.30 \le \eta \le 0.55$, although both are surpassed to some extent by the VF damper behavior in this range. On the other hand, when a larger reduction in drifts is desired, VE solutions and then finally BRB designs exhibit the best performance. Notice, however, the small additional reduction in drifts, which can be achieved by switching to these VE or BRB designs, is accompanied by a significant increase in accelerations, even beyond the level present in the bare frame.

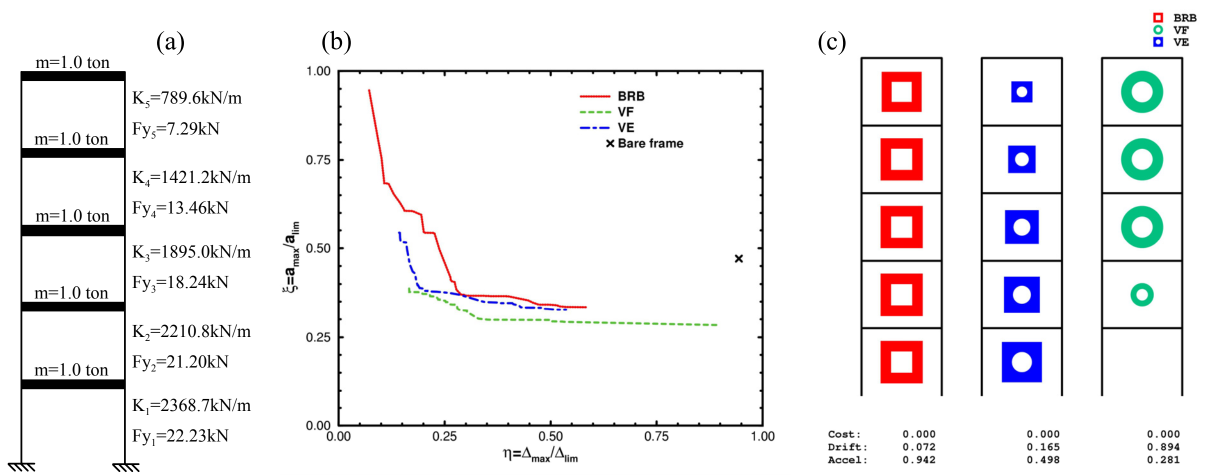

Figure 2 Five story yielding shear frame: (a) Model definition; (b) Pareto front for BRB, VF and VE dampers; (c) Optimal damper distributions

Several designs from the Pareto front curves in Figure 2b are examined in more detail. Figure 2c depicts the transition from BRB to VE to VF dampers discussed above for the case involving a single damper type. The left hand diagram is associated with the upper leftmost point on the Pareto front. This is the minimum drift design, which in this case, involves maximum size BRBs in all five stories. The middle diagram represents a point near the left hand end of the VE Pareto front. This too represents a low drift solution and is characterized by a nearly uniform drift distribution throughout the height of the building. Meanwhile, the rightmost diagram presents the minimum acceleration Pareto front solution, which has an inverted VF damping distribution (*i.e.*, large dampers in the upper stories and little or no added damping on the lower levels). This minimum acceleration Pareto solution produces nearly uniform story accelerations for the earthquake ensemble.

Next, the performance of NVF dampers is investigated by considering the effect of the exponent ν and brace stiffness factor κ. Figure 3a depicts the Pareto front for the case with $\nu = 1.0$, which represents the case of linear viscous dampers. The individual curves illustrate the effect of brace stiffness with the solid black line corresponding to a brace of infinite stiffness. As can be seen, performance improves as the brace stiffness increases. Meanwhile, Figure 3b illustrates Pareto fronts for nonlinear viscous fluid dampers with $\nu = 0.6$. Notice again that performance improves with increasing brace stiffness. However, now there are low drift, low acceleration solutions for the given range of nonlinear dampers with $\nu = 0.6$ and stiff braces. Similar results are obtained for NVF dampers with $\nu = 0.2$, as shown in Figure 3c. Damper distributions for the three cases with $\kappa = 10$ are provided in Figure 4. Finally, Figure 3d presents results for cases with an extended range of damper sizes to four times the original limit. Notice, in particular, that with the inclusion of larger dampers, even the linear VF can attain low drift, low acceleration solutions.

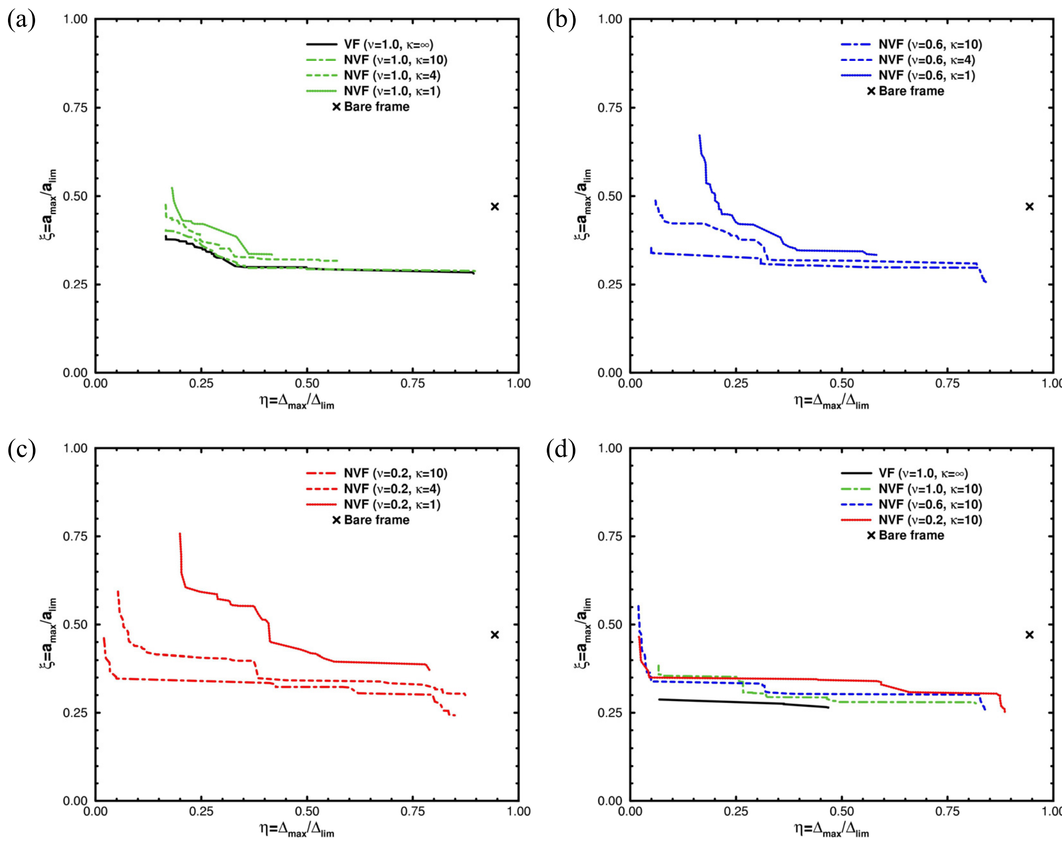

Figure 3 Five story yielding shear frame: (a) Pareto front for NVF with $\nu = 1.0$ and variable κ; (b) Pareto front for NVF with $\nu = 0.6$ and variable κ; (c) Pareto front for NVF with $\nu = 0.2$ and variable κ; (d) Pareto front for NVF with extended damper range and $\kappa = 10$

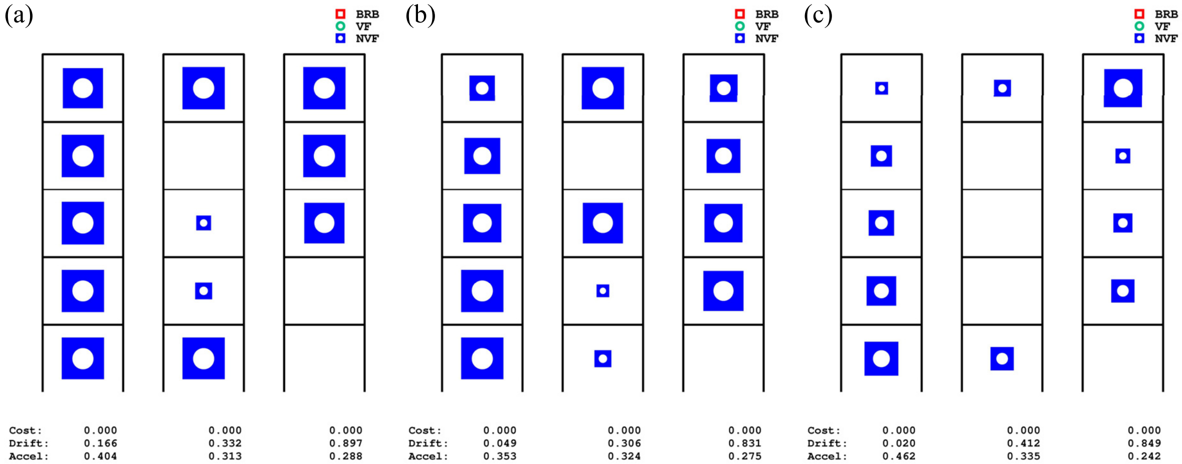

Figure 4 Five story yielding shear frame Pareto front damper distributions for $\kappa = 10$: (a) NVF with $\nu = 1.0$; (b) NVF with $\nu = 0.6$; (c) NVF with $\nu = 0.2$

6. CONCLUSIONS

With the recognition of total accelerations as an additional performance measure for the response of structures under seismic loadings, a new approach for the multi-objective optimal design of seismic retrofitting has been presented. Although not described here, an advanced genetic algorithm for multi-objective optimization also has been developed in order to maintain a diverse Pareto front during the evolutionary process. By using a time-history analysis for the fitness evaluation, nonlinear structures with different types of energy dissipation devices can be considered. Here the focus has been on the performance of buckling restrained braces, linear and nonlinear viscous fluid dampers and viscoelastic dampers. The initial results presented in this paper show interesting trends in the choice of damping device type and their distribution. However, in order to generalize these results a more comprehensive study is needed with additional structures and seismic environments. Furthermore, in future work, cost could be taken as another objective leading to a three-dimensional objective space that could be very helpful for the decision maker.

REFERENCES

Bertero, V.V. (1997). Performance-based seismic engineering: a critical review of proposed guidelines. *Proceedings of the International Workshop on Seismic Design Methodologies for the Next Generation of Codes*, A.A. Balkema, Rotterdam.

Christopoulos, C. and Filiatrault, A. (2006). *Principles of Supplemental Damping and Seismic Isolation*. IUSS Press, Milan, Italy.

Dargush, G.F. and Sant, R.S. (2005). Evolutionary aseismic design and retrofit with passive energy dissipation. *Earthquake Engineering and Structural Dynamics*, **34**, 1601-1626.

Furuya, O., Hamazaki, H. and Fujita, S. (1998). Study on proper distribution of storey-installation type damper for vibration control of slender structures using genetic algorithm. *Proc., 1998 ASME/JSME Joint Pressure Vessels and Piping Conf.*, San Diego, **364**, 297-304.

Holland, J.H. (1975). *Adaptation in Natural and Artificial Systems*. University of Michigan Press, Ann Arbor, MI.

Lavan, O. and Levy, R. (2005). Optimal design of supplemental viscous dampers for irregular shear-frames in the presence of yielding. *Earthquake Engineering and Structural Dynamics*, **34**(8), 889-907.

Levy, R. and Lavan, O. (2006). Fully stressed design of passive controllers in framed structures for seismic loadings. *Structural and Multidisciplinary Optimization*, **32**(6), 485-498.

Liu, W., Tong, M. and Lee, G.C. (2005). Optimization methodology for damper configuration based on building performance indices. *Journal of Structural Engineering* (ASCE), **131**(11), 1746-1756.

Moreschi, L.M. and Singh, M.P. (2003). Design of yielding metallic and friction dampers for optimal seismic performance. *Earthquake Engineering and Structural Dynamics*, **32**(8), 1291-1311.

Pareto, V. (1927). *Manuel d'économie Politique*, Giard, Paris.

Press, W.H., Teukolsky, S.A., Vetterling, W.T. and Flannery, B.P. (1992). *Numerical Recipes in FORTRAN*, Cambridge University Press, Cambridge, UK.

Priestley, M.J.N. (2000). Performance based seismic design. *Proceedings of 12WCEE*, Auckland, New Zealand.

Singh, M.P. and Moreschi, L.M. (2001). Optimum seismic response control with dampers. *Earthquake Engineering and Structural Dynamics*, **30**(4), 553–572.

Singh, M.P. and Moreschi, L.M. (2002). Optimal placement of dampers for passive response control. *Earthquake Engineering and Structural Dynamics*, **31**, 955–976.

Somerville, P., Smith, N., Punyamurthula, S. and Sun, J. (1997). Development of ground motion time histories for Phase 2 of the FEMA/SAC steel project," Report No. SAC/BD-97/04 1997 and http://quiver.eerc.berkeley.edu:8080/studies/system/ground_motions.html

Soong, T.T. and Dargush, G.F. (1997). *Passive Energy Dissipation Systems in Structural Engineering*. Wiley, London.

Takewaki, I. (1997). Optimal damper placement for minimum transfer functions. *Earthquake Engineering and Structural Dynamics*, **26**(11), 1113-1124.

Villaverde, R. (1997a). Method to improve seismic provisions for nonstructural components in buildings. *Journal of Structural Engineering* (ASCE), **123**(4), 432-439.

Villaverde, R. (1997b). Seismic design of secondary structures: State of the art. *Journal of Structural Engineering* (ASCE), **123**(8), 1011-1019.

Zhang, R.H. and Soong, T.T. (1992). Seismic design of viscoelastic dampers for structural applications. *Journal of Structural Engineering* (ASCE), **118**, 1375 –1392.